Food Chemistry: X 22 (2024) 101499

Contents lists available at ScienceDirect

Food Chemistry: X

journal homepage: www.sciencedirect.com/journal/food-chemistry-x

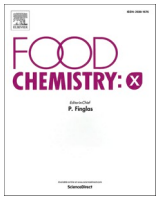

Accentuation of the browning characteristics and functional properties of aged tomatoes (*Solanum lycopersicum* cv.)

Yi-Chan Chiang, Po-Yuan Chiang *

Department of Food Science and Biotechnology, National Chung Hsing University, 145 Xingda Road, South Dist., Taichung City, 40227, Taiwan

ARTICLE INFO

Keywords:
Moisture-assisted aging technology
Biotransformation
α-Glucosidase inhibitory
Carotenoid oxidation product
Browning product

ABSTRACT

Moisture-assisted aging technology (MAAT) is a green process that improves browning characteristics and functionalities. This study investigated the physicochemical and functional characteristics of aged tomatoes. MAAT modulated carotenoids biotransformation from esterified to free form (Fourier-transform infrared spectroscopy 1738, 2851, and 2922 cm^{-1}) and generated primary and secondary oxidation volatiles, such as 4-terpineol, α-terpineol, and γ-terpineol (Headspace solid-phase microextraction gas chromatography-mass), which contributed woody and clove odors. Total flavonoids and α-glucosidase activity inhibitory were significantly increased from 1207.729 to 2318.204 mg RE/100 g DW and 77.703% to 86.851%, respectively. We discovered different synthesis pathways of 5-HMF and furfural under different water activities; this breakthrough may set furfural as an important factor in quality control of MAAT products in the future. Thus, MAAT can modulate the chemical form of tomato carotenoids, improve functionalities, and generate unique woody odor volatiles. These results may be applied to health food development in the food industry.

1. Introduction

Moisture-assisted aging technology (MAAT) is an additive-free, pollution-free, convenient, and rapid high-humidity thermal treatment technology that can modify the physical structure, texture, and flavor of foods. MAAT has been widely used in the food industry to extend the flavor and shelf life of food. Previous studies indicated that, differing from other green processing methods, such as high-pressure processing, MAAT widely overcomes the barriers of high cost and irregular food structure. (Wu, Jin & Zhang, 2021; Hsu, Yang, Chiang, Lin & Chiang, 2024). MAAT induces cell breakage to release the combined-form polyphenols in mature fruits and decomposes to release the phenols, enhancing antioxidant activities. In addition to deactivating enzymes, MAAT can also chemically transform phytochemicals, such as by cleaving glycosidic bonds, which can increase sweetness, reduce esterified phenol contents, and increase the low-molecular-weight free form phenolic acids (Juániz et al., 2016; Gan, Lui, Chan & Corke, 2017; Ríos-Ríos, Montilla, Olano & Villamiel, 2019). MAAT is affected by different temperatures, relative humidity, water activities, structural obstacles, and pH. Among these factors, the water activity level affects the reaction rate of non-enzymatic browning. Van Boekel (2001) have shown that higher water activity improves molecular mobility and enhances the Maillard reaction rate. In contrast, lower water activity increased the reactant concentration and decreased the diffusion reaction (Pakakaew et al., 2022).

Tomato (*Solanum lycopersicum* cv.) is an important fruit that has multiple varieties and not only has a unique sweet and sour flavor but also rich in carotenoids, polyphenols, polysaccharides, protein, dietary fiber, vitamins, and minerals. These components provide nutrients and have antioxidant, anti-inflammatory, antidepressant, and anti-cancer capacities (Khachik et al., 2002; Jomova & Valko, 2013). Carotenoids, including β-carotene, lutein, and lycopene, are widely present in plants. These compounds comprise multiple isoprene units. β-Carotene and lycopene are precursors of vitamin A and, similar to lutein, protect vision and the retina from light damage (Khachik et al., 2002). In addition, they neutralize free radicals in the body, reduce oxidative damage to cells, and achieve antioxidant effects. Previous studies have indicated that carotenoids have anti-inflammatory, anti-cancer, and immune-boosting functions (Jomova & Valko, 2013). However, when exposed to light, carotenoids are prone to isomerization, oxidation, and co-oxidation. In high-temperature and high-humidity environments, oxidation reactions degrade ascorbic acid, carotenoids, and enzymes, which lowers the antioxidant activities (Koh, Charoenprasert & Mitchell, 2012; Luterotti, Bicanic, Marković & Franko, 2015; Lu, Peng, Zhu &

* Corresponding author.
E-mail address: pychiang@dragon.nchu.edu.tw (P.-Y. Chiang).

https://doi.org/10.1016/j.fochx.2024.101499
Received 15 March 2024; Received in revised form 19 May 2024; Accepted 20 May 2024
Available online 23 May 2024

Table 1
Preparation of aged tomatoes by moisture-assisted aging technology.

Treatment	Blanching	HAD	MAAT
Condition	Boiled water bath, 5 min	65 °C, 12 h	65 °C, 75%RH, 12 days
Fresh			
UW			●
UD		●	●
BW	●		●
BD	●	●	●

*Abbreviation descriptions: HAD, MAAT, and RH represented the hot-air drying, moisture-assisted aging process, and relative humidity, respectively. U and B mean unblanched and blanched, respectively. W and D mean the samples used fresh or pre-dried tomatoes, respectively.
*"●" means the tomato sample group prepared included that treatment.

Pan, 2018). Climate change and infectious diseases have impacted human life in recent years, including greater uncertainty in crop production and demand, leading to food shortages (Mirón, Linares & Díaz, 2023). In the traditional functional diet of Asians, aged fruits and vegetables are common and popular.

Increasingly, Asian food markets focus on healthcare products developed by MAAT that are widely used, such as black garlic, black lemon, black apple, and aged orange. Black garlic is the most popular MAAT product. It is fermented at 60–80 °C and 60–80% relative humidity (RH) for eight weeks to reduce pungency, spiciness, and stomach-irritating organosulphur levels. This changes the chewy and rubbery texture and makes it sweeter by decomposing fructans. In addition, γ-glutamyltransferase can decomposite S-allylcysteine in black garlic to produce γ-glutamyl-s-allylsysteine during MAAT, which greatly increases the antioxidant properties (Pakakaew et al., 2022). The increase in antioxidant components and free phenols brings out better antioxidant activity, anti-inflammatory activity, lowering blood pressure, anti-cancer, and other physiological functions (Zanoni, Pagliarini, Giovanelli & Lavelli, 2003; Yilmaz & Toledo, 2005; Wu et al., 2021). The Maillard reaction generates the intermediate product 5-hydroxymethylfurfural (5-HMF), which is a good antioxidant that inhibits α-glucosidase activity, which lowers blood sugar levels in diabetics after meals (Zhang et al., 2023; Hsu et al., 2024).

Aged tomatoes (AT) are well-liked by consumers, have an attractive flavor and texture, and are rich in phytochemicals. However, no work has evaluated the development and quality of research on tomatoes with higher water activity. It is important to develop and investigate functional AT through green processing, which has the advantages of being natural and free of additives. However, among the Maillard reaction products (MRPs), not only 5-HMF but also furfural can be synthesized in acidic environments and should be set as quality indices during MAAT (Carvalho, de Oliva Neto, Da Silva & Pastore, 2013). However, no previous study has mentioned the synthesis pathway of these two MRPs in MAAT products so far. Thus, this study aimed to investigate the AT produced from tomatoes with different water activities by MAAT at 65 °C and 75% RH for 12 days. Using principal component analysis (PCA) to find out the changes in physicochemical properties (like color, water activity, pH, carotenoid content, FTIR spectra, and volatile composition) and functionalities (like total polyphenol content, total flavonoid content, DPPH free radical scavenging rate, FRAP iron reduction power, and α-glucosidase inhibition rate). We also used heatmap analysis to infer the pathway of browning reaction regulation, which synthesizes 5-HMF and furfural. These results will serve as quality references for developing functional AT in the future.

2. Materials & methods

2.1. Materials and chemicals

Fresh beef tomatoes (*Solanum lycopersicum* cv.) were purchased from Taiding Automatic Co. Ltd. (Taichung, Taiwan), and each weight was approximately 105 ± 15 g. These tomatoes were delivered, selected, washed, and cooled at room temperature (25 ± 5 °C). All chemicals used were of analytical grade from Sigma-Aldrich Co. (Missouri, USA). All solutions were prepared using deionized water with a resistivity of no $<18.2\ M\Omega\ cm^{-1}$.

2.2. Preparation of aged tomato

In this study, tomatoes were separated into five groups. Different process conditions were shown in Table 1. A dehydrator (Model 3926 TB, Excalibur Dehydrator Co., CA, USA) was used for hot-air drying (HAD), and a temperature humidity chamber (Model BTH80/−20, Firstek Co., New Taipei, Taiwan) was used for the moisture-assisted aging technology (MAAT).

The fresh group represented the fresh tomato samples, and there were four aged tomato groups. The UW group was processed by MAAT directly, which was carried out within 12 days under 65 °C and 75% relative humidity (RH) conditions. The sole distinction between BW and UW was in the application of a 5-min blanching treatment within a boiled water bath. UD group was carried out by HAD and MAAT processes; HAD adjusted the water activity to approximately 0.607–0.719 under 65 °C for 12 h. After that, MAAT with the same condition was set at 65 °C and 75% relative humidity for 12 days.

2.3. Quality indices of aged tomato

2.3.1. Appearance

A stereoscopic dissecting microscope (Model SMZ800, Nikon Co., Tokyo, Japan) and a digital single-lens reflex camera (Model 450D, Canon Co., Tokyo, Japan) worked together to capture the surface images of the microstructures.

2.3.2. Water activity

The water activity of AT was measured with a water activity meter (Model Aqualab 3TE, Meter Group Inc., WA, USA).

2.3.3. Color measurement and color difference calculation

The lightness value (L*), red/green coordinate (a*), and yellow/blue coordinate (b*) of AT were measured with a color meter (Model ZE-2000, Nippon Denshoku Industries Co., Tokyo, Japan) and calibrated with a standard whiteboard (X = 92.81, Y = 94.83, Z = 111.71) and a zero box. The calculation of the color difference followed the formula below (Eq. 1).

$$\textit{Colour Difference}\ (\Delta E) = \sqrt{\left(L_1^* - L_0^*\right)^2 + \left(a_1^* - a_0^*\right)^2 + \left(b_1^* - b_0^*\right)^2} \quad (1)$$

2.3.4. pH value

The pH value of AT was measured with a pH meter (Model SP-2300, Suntex Instruments Co., New Taipei, Taiwan) after three-point calibration (pH 4, 7, and 10).

2.3.5. Browning degree measurement

The AT extracts were the same as ***2.4.2.***. The browning degree measurement was the absorbance value at 420 nm (A420) using a microplate reader (Model SPECTROstar Nano, BMG Labtech Co., Ortenberg, Germany).

2.4. Browning reaction component analysis

2.4.1. Ascorbic acid contents

1 g of dried sample powder was mixed with 10 mL of 70% LC-grade ethanol. The extraction used an ultrasonic vibrator for 30 min at room temperature (25 ± 5 °C) in a dark environment and passed the 0.2 μm PTFE filter (Waters Co., Milford, USA) to ensure no precipitation existed before high-performance liquid chromatography with diode array

detector (HPLC-DAD) analysis. An HPLC-DAD is composed of an auto-sampler (Model PN5300, Postnova Co., Utah, USA), a chromatographic pump (Model Chromaster 5110, Hitachi Co., Tokyo, Japan), a Mightysil RP-18GP column (250 mm, 4.6 mm i.d., 5.0 μm) (Kanto Co., Tokyo, Japan), and a diode-array detector (Model L-2450, Hitachi Co., Tokyo, Japan). The mobile phase used the same gradient of 0.02 M ammonium dihydrogen phosphate buffer (pH 2.2 ± 0.2) in double-distilled water and was analyzed for 20 min. 10 μL of samples were injected with 1.00 mL/min flow rate of mobile phase at 25 °C. The DAD detection wavelength was set at 243 nm. Ascorbic acid was identified by comparing the retention time (min) of standards and quantified to dried weight (mg/g) by calibration curves from standards as well.

2.4.2. Sugar composition analysis

2 g of dried sample powder was mixed with 10 mL of double-distilled water. The extraction used an ultrasonic vibrator for 30 min at room temperature (25 ± 5 °C) in a dark environment and passed the 0.2 μm PTFE filter to ensure no precipitation existed before high-performance liquid chromatography with refractive index detector (HPLC-RI) analysis. The HPLC system used the same as ***2.4.1.***, except the column and detector used a Shodex RSpak DC-613 column (150 mm, 6 mm i.d.) (Kanto Co., Tokyo, Japan), and a refractive index detector (Model 5450, Hitachi Co., Tokyo, Japan), respectively.The mobile phase used the same gradient of LC-grade acetonitrile with 1.5 mM NaOH in double-distilled water and was analyzed for 20 min. 10 μL of samples were injected with a 1.50 mL/min flow rate of mobile phase at 70 °C. Sucrose, fructose, and glucose were identified by comparing the retention time (min) of standards and quantified to dried weight (mg/g) by calibration curves from standards as well.

2.4.3. 5-Hydroxymethylfurfural and furfural analysis

The sample extraction method and HPLC-DAD parameter was followed by ***2.4.1.***. The mobile phase used the same gradient of 12% acetonitrile in double-distilled water and was analyzed for 20 min. 15 μL of samples were injected with 1.00 mL/min flow rate of mobile phase at 25 °C. The DAD detection wavelength was set at 284 nm. 5-Hydroxymethylfurfural (5-HMF) and furfural were identified by comparing the retention time (min) of standards and quantified to dried weight (mg/g) by calibration curves from standards as well.

2.5. Carotenoids composition analysis

Followed and modified by Lu et al. (2018), weighted 2 g of dried sample powder was mixed with 20 mL of LC-grade ethyl acetate. The extraction used an ultrasonic vibrator for 30 min at room temperature (25 ± 5 °C) in a dark environment and passed the 0.2 μm PTFE filter to ensure no precipitation existed before HPLC-DAD analysis. The HPLC-DAD parameter was followed by ***2.4.1.***. The mobile phase gradients of A (75% methanol in double-distilled water) and B (ethyl acetate) were run starting from 70% A, then increased to 90% A in 11.5 min, decreased to 30% A in the next 3.9 min, and held for 3.8 min, increased to 70% A for the next 3.9 min, and kept for the final 3.9 min. 15 μL of samples were injected with 1.00 mL/min flow rate of mobile phase at 25 °C. The DAD detection wavelength was set at 450 nm. Lutein, lycopene, and β-carotene were identified by comparing the retention time (min) of standards and quantified to dried weight (mg/g) by calibration curves from standards as well.

2.6. Fourier-transform infrared spectroscopy analysis

Followed by Yuan, Chiang, Li and Chiang (2024), all AT samples were analyzed by a Fourier-transform infrared spectrometer (FTIR) (Model Nicolet 6700, Thermo Fisher Scientific Co., MA, USA) and MCT detector (Thermo Fisher Scientific Co., MA, USA). The scanning range was from 650 to 4000 cm^{-1}. Spectra were collected, and the resolution was set at 2 cm^{-1}/30 s.

2.7. Antioxidant contents and activities analysis

The sample extraction method was followed by ***2.4.1.***.

2.7.1. Total polyphenol contents

Followed and modified the method by Hsu et al. (2024), 70 μL of the AT extracts were added into equal volumes of the Folin-Ciocalteu reagent, then vortexed and stored in a dark environment for 3 min. In addition, 35 μL of 10% Na_2CO_3 was stored in double-distilled water and stored for 30 min after vortexing. The absorbance value was determined at 735 nm using a microplate reader (Model SPECTROstar Nano, BMG Labtech Co., Ortenberg, Germany). Gallic acid was used as the standard and quantified to dried weight (mg/g) by calibration curves.

2.7.2. Total flavonoid contents

Followed and modified the method by Ciou, Chen, Chen and Yang (2021), 10 μL of the AT extracts were added into 60 μL of the double-distilled water, then added the 30 μL 5% $NaNO_2$ in double-distilled water and stored under a dark environment for 6 min. In addition, 25 μL of 25% $AlCl_3$ was stored in double-distilled water, 25 μL of 2% NaOH was stored in double-distilled water, and 50 μL of double-distilled water was stored for 15 min after vortex. The absorbance value was determined at 415 nm using a microplate reader. Quercetin was used as the standard and quantified to dried weight (mg/g) by calibration curves.

2.7.3. 2,2-Diphenyl-1-picrylhydrazyl (DPPH) radical scavenging activity

Followed and modified the method by Li, Shih, Lu, Huang and Wang (2023), 10 μL of the AT extracts were added into 40 μL of the 100 mM Tris-HCl buffer (pH 7.4), then added 75 μL of 0.5 mM DPPH in LC-grade methanol and stored under a dark environment for 30 min. The absorbance value (A) was determined at 517 nm using a microplate reader. Trolox was used as the standard and quantified to dried weight (mg/g) by calibration curves. The calculation of the scavenging rate of the samples was followed by the formula below (Eq. 2).

$$DPPH\ (\%) = \frac{(A_{blank} - A_{sample})}{(A_{blank})} \times 100 \quad (2)$$

2.7.4. Ferric ion reducing antioxidant power (FRAP)

Followed and modified the method by Li et al. (2023), the FRAP reagent was composited with 300 mM acetate buffer (pH 3.6), 10 mM TPTZ in 40 mM HCl, and 20 mM $FeCl_3$ in double-distilled water at a ratio of 10:1:1. 20 μL of the AT extracts were added to 150 μL of the FRAP reagent and stored in a dark environment for 10 min at 37 °C. The absorbance value was determined at 593 nm using a microplate reader. Trolox was used as the standard and quantified to dried weight (mg/g) by calibration curves.

2.8. In vitro α-glucosidase inhibitory capacity

Followed and modified the method by Hsu et al. (2024), 50 μL of the AT extracts were mixed with 100 μL of the α-glucosidase diluent (approximately 1.000 U/mL), and then 50 μL of p-NPG was added. The mixture was kept in the dark for 5 min at room temperature (25 ± 5 °C). The absorbance value was determined at 400 nm using a microplate reader. 7 mg of acarbose was diluted with 100 mL of 70% ethanol and used as the positive control to convert the inhibitory capacity of the AT extracts. The background group was composed of 50 μL of the AT extracts, 100 μL of PBS solution, and 50 μL of p-NPG. The PBS solution was composited with 7.7 g NaCl, 0.7 g Na_2HPO_4, and 0.2 g KH_2PO_4 in double-distilled water, then adjusted to pH 7.4 by 1 N NaOH in HCl. The calculation of the inhibitory rate of samples followed the formula below (Eq. 3).

$$\alpha - Glucosidase\ inhibitory\ (\%) = \frac{A_{sample} - A_{background}}{A_{acarbose} - A_{background}} \times 100 \quad (3)$$

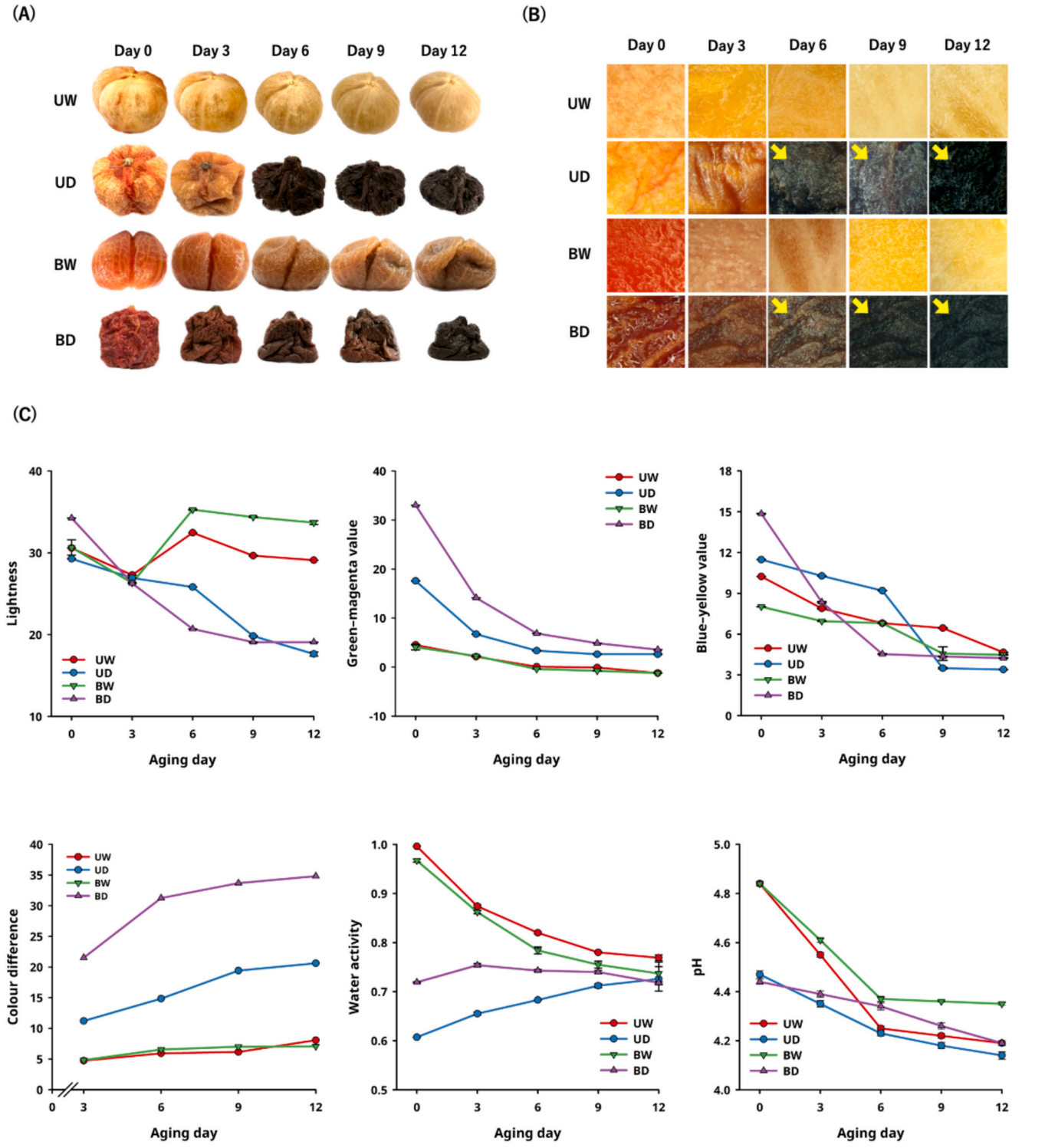

Fig. 1. Effects of physical properties on tomatoes during moisture-assisted aging technology. (A) Visual appearance (B) Surface microstructure (C) Color analysis, color difference, water activity, and pH.
*Abbreviation description: U and B mean unblanched and blanched, respectively. W and D mean the samples used fresh or pre-dried tomatoes, respectively.

2.9. Headspace solid-phase microextraction gas chromatography–mass spectrometry analysis

Followed and modified by Tsai et al. (2021) and Lin, Chen, Chen, Chen and Yang (2024), 10 mL of aged tomato extracts by ***2.4.2.*** and added 1 μL of 20 ppm ethyl decanoate as an internal standard in each sample. Then settle the BT extracts in a 20-mL headspace vial (Thermo Fisher Scientific Co., Waltham, Massachusetts, USA). Extracted by multifunctional autosampler system AOC-6000 (PAL system Co., Zwingen, Switzerland) combined with SPME-Arrow Tool (PAL system Co., Zwingen, Switzerland) for 10 min at 60 °C, then used DVB/PDMS fiber (120 μm/20 mm) (PAL system Co., Zwingen, Switzerland) to extract for 10 min.

All samples were analyzed by the gas chromatography model GC-

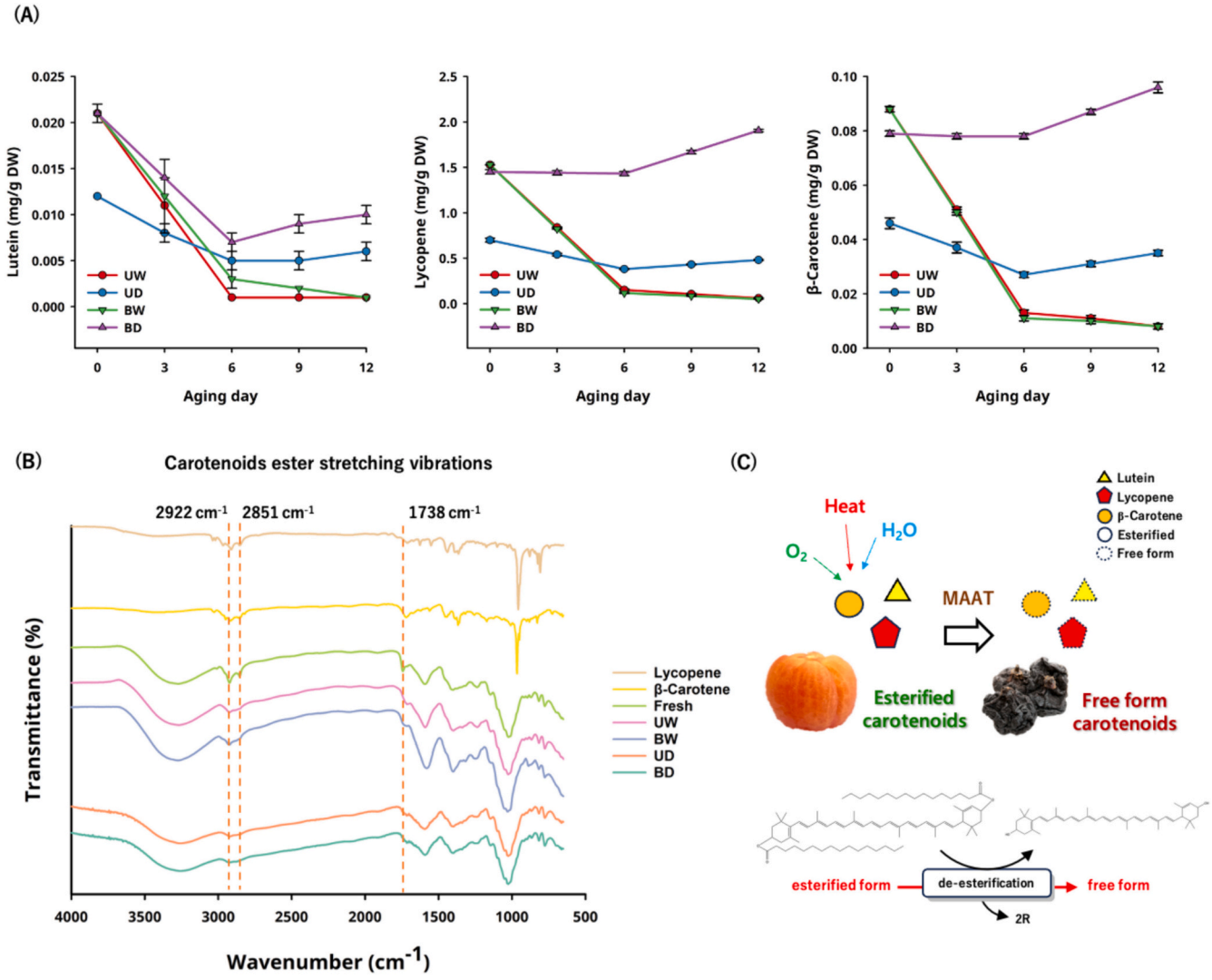

Fig. 2. Effects of carotenoid contents on tomatoes during moisture-assisted aging technology. (A) Carotenoid contents (B) Fourier-transform infrared spectra (C) Schematic diagram of the speculated mechanism.
*Abbreviation description: U and B mean unblanched and blanched, respectively. W and D mean the samples used fresh or pre-dried tomatoes, respectively.

2010 Plus using the SH-Rxi-5Sil-MS column (30 m × 0.25 mm i.d. × 0.25 μm) combined with the mass spectrometry model GCMS-TQ8040 from Shimadzu Co. (Kyoto, Japan) to isolate different volatile compounds. The initial temperature of the oven was 40 °C and held for 1 min, then gradually increased to 200 °C at the rate of 4 °C/min and increased to 240 °C at the rate of 80 °C/min and held for 3 min. Sample injection time was 1 min with a flow rate of 1 mL/min of 99.9995% helium gas (Dry Ice Technology Co., Chiayi, Taiwan) as the mobile phase. The mass spectrometer was operated in electron ionization mode (positive ion, 70 eV). The ion source was settled at 200 °C and mass spectra were acquired in full scan from 40 to 400 *m/z*. The retention index (RI) was calculated from the retention time (RT) of *n*-alkanes by Automatic Adjustment of Retention Time standards (AART) (Shimadzu Co., Kyoto, Japan). The RI and mass spectrogram of volatile compounds were identified by comparing the databases of the FFNSC 3 library (Shimadzu Co., Kyoto, Japan) and the NIST 2018 library (The National Institute of Standards and Technology, Maryland, USA), and the relative contents were quantified based on the peak area of the compound over the peak area of the internal standard (C/I) (Eq. 4).

$$\textit{Relative content}\ (C/I) = \frac{\textit{peak area of volatile}}{\textit{peak area of internal standard}} \quad (4)$$

2.10. Statistical analysis

All results were shown as mean ± standard deviation in the database ($n = 3$). Data were collected by the one-way analysis of variance (ANOVA) of SPSS version 12.0 software (IBM Co., Armonk, New York, USA). Significance tests were determined by Duncan's multiple range test (DMRT), and all comparisons were considered statistically significant if $p < 0.05$. The principal component analysis (PCA), agglomerative hierarchical clustering (AHC), and heatmap analysis were exported with XLSTAT software (Addinsoft Co., New York, USA).

3. Results and discussion

3.1. Aging appearance of aged tomatoes

The color of fresh tomato pulp is commonly yellow and red, mainly due to lutein, lycopene, and β-carotene. After aging at 65 °C and 75% RH for 12 days, a browning reaction occurred in all samples, while in the lower water activity groups, that is, the UD and BD groups, a dark brown-black color resulted (Fig. 1A). The tomato groups without blanching (UW and UD) may undergo enzymatic and non-enzymatic browning. The blanched group, on the other hand, was mostly

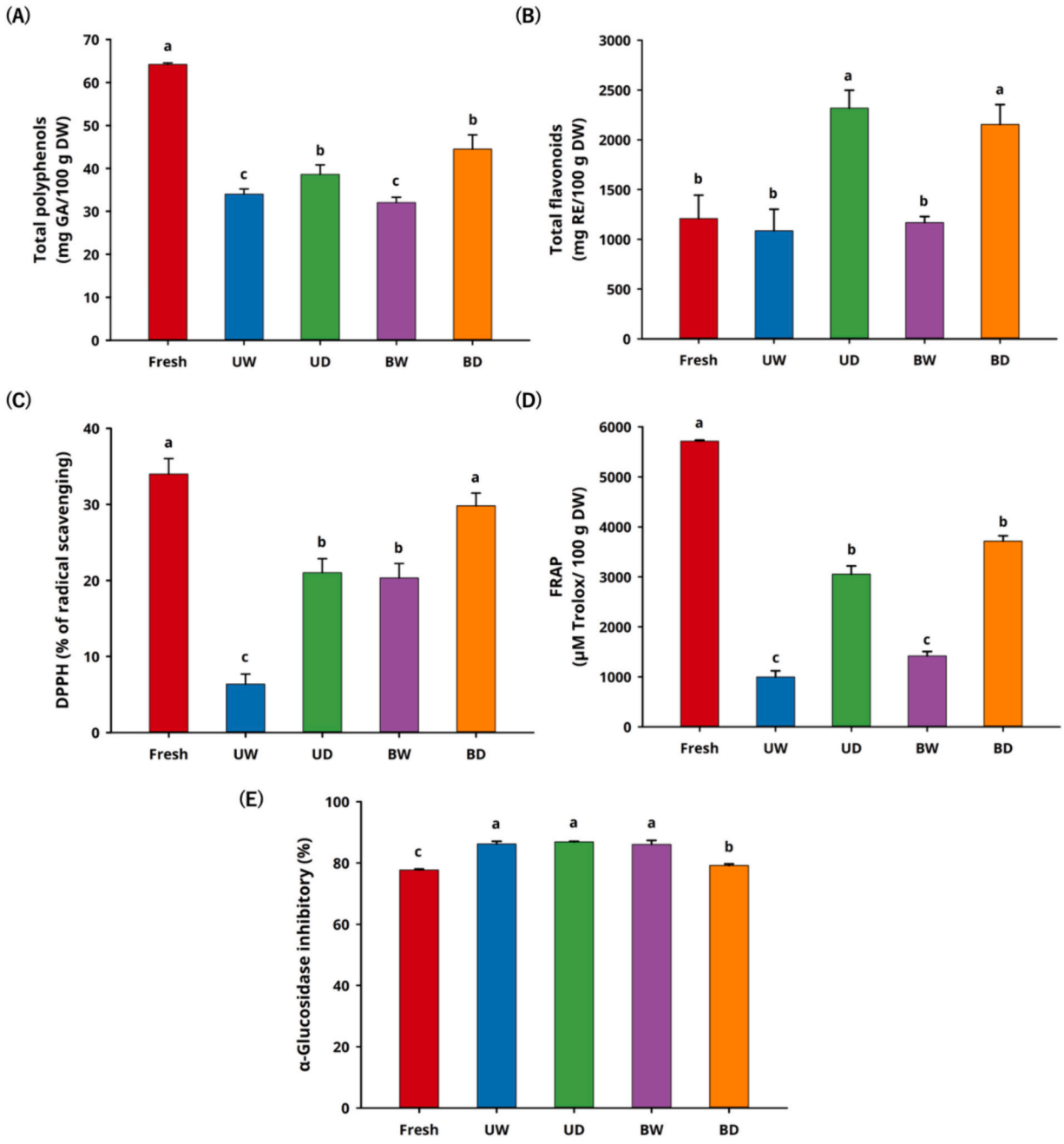

Fig. 3. Effects of in vitro bio-functional properties on tomatoes during moisture-assisted aging technology. (A) Total polyphenol contents (B) Total flavonoid contents (C) DPPH (D) FRAP (E) α-Glucosidase inhibitory.
*Abbreviation description: U and B mean unblanched and blanched, respectively. W and D mean the samples used fresh or pre-dried tomatoes, respectively.

browning without enzymes and building up browning products, which made it less light-transparent and gave it a dark brown-black color. The texture softened as the aging time increased, and the structural decomposition occurred in groups UD and BD. According to previous studies, the thermal treatment caused structural tissue decomposition, which led the bioactive substances out of the cell and made the material stickier and chewier (Pakakaew et al., 2022; Hsu et al., 2024). In Figs. 1B–C, a dark brown color was observed in the lower water activity groups (UD and BD). The water activity increased from 0.607 to 0.719 to 0.718–0.726 to achieve a stable balance, while in the higher water activity groups, it decreased from 0.967 to 0.996 to 0.737–0.769. The reaction rate of the non-enzymatic browning was highest at a water activity between 0.600 and 0.800, as mentioned in previous studies (Van Boekel, 2001; Pakakaew et al., 2022).

In the color analysis results shown in Fig. 1C, the L* of the higher water activity groups (UW and BW) increased to 26.33–27.29 on the third day and increased to 25.82–32.46 on the sixth day of aging. This contributed to the degradation of the natural red pigment in the AT and improved L*. The L* of the low water activity group showed a decreasing trend from 29.28 to 34.25 to 17.63–19.08, and the surface of the AT was observed through a microscope at 20 times magnification to be dense and wrinkled (Fig. 1B). In all AT groups, a* and b* showed a regular decreasing trend, with a* and b* decreasing to −1.22–3.56 and 3.39–4.65, respectively, after 12 days of MAAT, indicating a decrease in redness and yellowness. Color difference (ΔE) is often used to evaluate the degree of color difference. Compared to fresh tomatoes, the ΔE of the group BD, which has blanched and pre-dried treatment, increased the most during MAAT, followed by UD > UW ≈ BW. According to a

previous study, adjusting the water activity to approximately 0.600–0.700 can accelerate the browning reaction under MAAT (Fig. 1C) (Van Boekel, 2001; Pakakaew et al., 2022; Hsu et al., 2024).

The pH of fresh tomatoes decreased from 4.44 to 4.84 to 4.14 to 4.35 after 12 days of MAAT (Fig. 1C). This might be because 5-HMF and furfural are acidic MRPs and are found in an acidic condition. (Liu et al., 2022). The organic acids released from the internal structure caused a sour flavor. The MRPs are generally considered to have no benefit to human health. However, 5-HMF is a common compound with advantages because of its antioxidant activities and is normally present in foods consumed daily, such as roasted wheat flours, black garlic, black apple, and aged orange. It provides beneficial daily doses due to its antioxidant activities and α-glucosidase inhibitory features (Wu et al., 2021; Zhu et al., 2022; Zhang, Guo, et al., 2023; Zhang, Tong, et al., 2023; Hsu et al., 2024).

3.2. Carotenoid content changes in aged tomatoes

Carotenoids were abundant phytochemicals in AT, mainly composited with lycopene, β-carotene, and lutein, with functional and healthcare characteristics. Esterified tomato pigments are more common in plant cells because of their stability. These carotenoids dissolve more easily in lipids and fit into the membrane structure more easily (Minguez-Mosquera & Hornero-Mendez, 1994). The HPLC-DAD result showed that the lutein, lycopene, and β-carotene contents of the AT were 0.021 ± 0.007, 1.528 ± 0.002, and 0.088 ± 0.001 mg/g DW (Fig. 2A). The content of lutein, lycopene, and β-carotene in the UD group decreased by 95.24%, 96.07%, and 90.91%, respectively, after predrying at 65 °C for 12 h. This decrease is due to the accelerated lipoxygenase oxidation of tomatoes (Gupta, Kopec, Schwartz & Balasubramaniam, 2011), which reduces the level of carotenoids. In contrast, blanching the AT before hot-air drying can effectively inhibit the enzymatic reaction, maintain carotenoid contents, and reduce water activity.

The carotenoid content in Fig. 2A decreased significantly until the sixth day of MAAT for the higher water activity groups (UW and BW), but it increased for the lower water activity groups (UD and BD). According to previous research on black garlic, black apple, and aged orange, the aging process increased the decomposition of macromolecular polyphenols and the content of smaller molecules of free form phenols, leading to higher antioxidant activity (Wu et al., 2021; Zhu et al., 2022; Hsu et al., 2024). The BD group also had higher contents of lycopene and β-carotene after 12 days of MAAT, at 1.906 ± 0.014 mg/g DW and 0.096 ± 0.002 mg/g DW, respectively. These contents were 24.74% and 9.09% higher than the fresh ones. This shows that lowering the water activity of substrates can decompose tissue structure during the aging process and make more bioactive ingredients available (Hsu et al., 2024).

Samples analyzed using FTIR spectroscopy included Fresh, UW, BW, UD, BD, and lycopene and β-carotene standards (Fig. 2B). The characteristic peaks of water were observed in the range of 3000–3500 cm^{-1} with wide bands and also detected at 1619 cm^{-1} (Dedić & Alispahic, 2017). The characteristic peaks of carotenoid esters in tomatoes have been mentioned in previous studies, mainly characterized by the stretching vibration of ester bonds at 2922, 2851, and 1738 cm^{-1} (Dedić & Alispahic, 2017; Iqbal et al., 2023). The groups with lower water activity (UD and BD) showed a reduced vibrational stretching peak of the carotenoid ester bond compared to the groups with higher water activity (UW and BW). This meant that tomatoes with less water activity accelerated the chemical bond breaking of carotenoids, which led to a higher ratio of free form carotenoids (Fig. 2C) (Lu et al., 2018). Previous studies have determined that appropriate thermal treatment can convert the forms of carotenoids, similar to the conversion of the esterified form and lutein in free form in wheat grains at 80 °C and the free form carotenoids enhanced the thermal stability of orange juice after thermal treatment. These studies proved that the improvement was caused by the phytochemicals and their changed chemical bonds in the food structure (Ahmad, Asenstorfer, Soriano & Mares, 2013; Lu et al., 2018).

3.3. Antioxidant contents, activities, and in vitro α-glucosidase inhibition of aged tomatoes

Antioxidant capacity and its health benefits play important roles in the human diet, such as improving immune system function, having anti-aging effects, and preventing chronic diseases (e.g., heart disease or cancer). The antioxidant components in fresh tomatoes include ascorbic acid, carotenoids, polyphenols, and flavonoids, which are good free radical scavengers. To evaluate the antioxidant properties of AT after MAAT for 12 days, the total polyphenol contents, total flavonoid contents, DPPH free radical scavenging capacity, and ferric-reducing antioxidant power were investigated.

The total polyphenol levels in the AT were significantly lower ($p < 0.05$) in Fig. 3A. The contents were approximately 64.184 ± 0.344 mg GA/100 g DW in the fresh group, 32.049–34.023 mg GA/100 g DW in the higher water activity groups (UW and BW), and 38.615–44.505 mg GA/100 g DW in the low water activity groups (UD and BD). This result differs from the results of black garlic but is similar to black apple and aged orange (Wu et al., 2021; Zhu et al., 2022; Hsu et al., 2024). When the rate of polyphenol decomposition is less than the low-molecular-weight phenolic acid consumption rate, the total polyphenol content will be reduced. The lower water activity group contained less free water, which reduced the reaction base and maintained a higher total polyphenol contents than the higher water activity groups ($p < 0.05$). These results also showed that the lower water activity of black garlic can not only decrease the non-enzymatic browning reaction rate but also maintain a higher polyphenol content. Tomatoes are considered an important source of flavonoids, especially contain approximately 30% free form quercetin. In addition, previous studies have indicated that thermal processing can decompose the tomatoes cell tissue and transform into free form flavonoids (Jacob, Garcia-Alonso, Ros & Periago, 2010). In Fig. 3B, the total flavonoid contents of AT significantly increased in the lower water activity groups (UD and BD), from 1207.729 ± 236.503 mg RE/100 g DW to 2154.472–2318.204 mg RE/100 g DW ($p < 0.05$). This phenomenon may be attributed to the increased non-enzymatic browning reaction in lower water activity-based tomatoes (Van Boekel, 2001; Pakakaew et al., 2022), effectively disintegrating the tomato cell tissue, thereby generating more free form flavonoids. Flavonoids, such as rutin and quercetin, do not change much when heated, so there was not a big difference in the content of flavonoids in the fresh tomatoes compared to the higher water activity groups (UW and BW) ($p > 0.05$) (Gahler, Otto & Böhm, 2003; Jacob et al., 2010).

The antioxidant activity results are shown in Figs. 3C–E. The DPPH and FRAP antioxidant activities of fresh tomatoes were approximately 33.994 ± 2.053% and 5715.476 ± 19.085 μM Trolox/100 g DW, respectively. Related to the total polyphenol contents, the decreasing trend in the antioxidant capacities of the AT occurred in both the DPPH and FRAP assays, which may also be attributed to the significant reduction of ascorbic acid (Koh et al., 2012; Luterotti et al., 2015). The DPPH and FRAP antioxidant activities of the AT in group BD were relatively higher than the other groups, with 29.822 ± 1.666% and 3717.073 ± 106.315 μM Trolox/100 g DW, which were reduced by 12.27% and 34.96%, respectively. There is no significant difference when group BD was compared to fresh tomatoes ($p > 0.05$). This result may be attributed to the higher content of polyphenols and MRPs, and MRPs have been reported to have antioxidant capacities in foods with thermal treatments (Zanoni et al., 2003; Yilmaz & Toledo, 2005; Zhang, Guo, et al., 2023; Zhang, Tong, et al., 2023; Hsu et al., 2024).

α-Glucosidase mainly reacts in the small intestine villi and raises the level of monosaccharide by decomposing polysaccharides. This raises blood sugar levels, which is a big challenge for diabetic patients. 5-HMF, one of the MRPs, can inhibits α-glucosidase activity (Hsu et al., 2024). We evaluated the inhibitory activity of fresh tomatoes and AT samples.

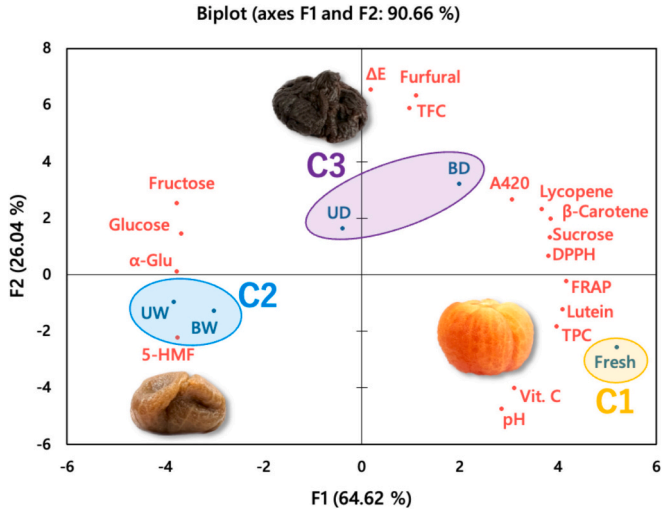

Fig. 4. Principal component analysis blots of overall change of aged tomato after 12-day moisture-assisted aging technology.
*Abbreviation description: U and B mean unblanched and blanched, respectively. W and D mean the samples used fresh or pre-dried tomatoes, respectively.

Fresh tomatoes and AT samples were approximately 77.703 ± 0.310% and 79.204–86.851%, respectively. This showed similar results to our previous study, the inhibitory rates of the higher water activity groups (UW and BW) containing 5-HMF significantly increased ($p < 0.05$) (Fig. 4) (Hsu et al., 2024). In the lower water activity groups (UD and BD), AT had a better α-glucosidase inhibition effect, which may be due to the increased total flavonoid contents (Li et al., 2018). The preliminary results confirm that AT could be a potential dietary ingredient for blood sugar control in people with diabetes.

3.4. Overall changes to aged tomatoes

In order to explore the changes in the physicochemical characteristics and functional properties of AT with different water activity groups after 12 days of MAAT, PCA was performed to explain the relationship between the components of the AT. The color difference value (ΔE), pH, browning degree (A420), sugars (sucrose, glucose, and fructose), ascorbic acid (Vit. C), browning products (5-HMF, furfural), carotenoids (lycopene, β-carotene, and lutein), total polyphenol content (TPC), total flavonoid content (TFC), free radical scavenging ability (DPPH), ferric reducing antioxidant power (FRAP), and α-glucosidase activity inhibitory (α-Glu) were analyzed in Fig. 4. After agglomerative hierarchical clustering (AHC) analysis, fresh tomatoes (C1: fresh), high water activity groups (C2: UW & BW), and lower water activity groups (C3: UD & BD) were divided into three clusters with significant differences ($p < 0.05$). Principal components F1 and F2 represent 64.62% and 26.04% of the overall data, respectively; the total, 90.66%, indicated good representativeness.

In Fig. 4, fresh tomatoes were classified as C1 and located on the right side of the PCA plot. Higher antioxidant activities were attributed to higher ascorbic acid and polyphenol contents, which decompose after MAAT. The higher water activity of AT was classified as C2 and was located on the left side of the PCA plot. This meant that the glycosidic bond of sucrose in fresh tomatoes was broken, which raised the levels of glucose and fructose, making the tomatoes sweeter. In addition, higher 5-HMF content and *in vitro* α-glucosidase activity inhibitory in C2 (Hsu et al., 2024). AT from lower water activity-based tomatoes were classified as C3 and have significantly increased total flavonoid contents, furfural contents, and color difference values. The increase in furfural might be because of ascorbic acid oxidation (Carvalho et al., 2013; Wallington, Clark, Prenzler, Barril & Scollary, 2013), and the

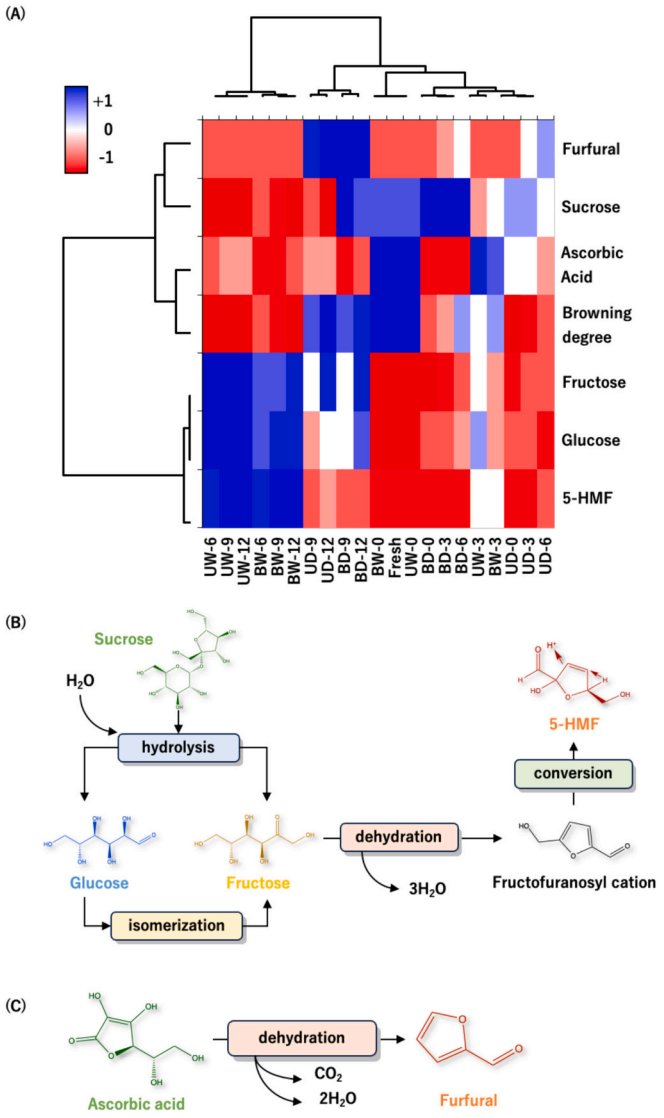

Fig. 5. Effects of browning model characteristics on tomatoes during moisture-assisted aging technology. (A) Heatmap (B) 5-HMF formation pathway (C) Furfural formation pathway.
*Abbreviation description: U and B mean unblanched and blanched, respectively. W and D mean the samples used fresh or pre-dried tomatoes, respectively.
*The number after "-" means aging day.

antioxidant activity is raised by the browning products synthesis during thermal treatment (Zanoni et al., 2003; Yilmaz & Toledo, 2005). Group BD and fresh tomatoes had no significant difference in carotenoid contents or antioxidant activities. After MAAT, the esterified form was reduced, and the free form increased. AT may have antioxidant properties because it has more free form flavonoids and MRPs, which have been reported in previous studies (Zanoni et al., 2003; Yilmaz & Toledo, 2005; Juániz et al., 2016; Gan et al., 2017; Ríos-Ríos et al., 2019). The PCA plot indicates that water activity was a critical reaction substrate and regulated different browning reaction pathways during MAAT. However, this result requires further clarification of the browning reaction pathways of AT.

3.5. Browning reaction mechanism affected by water activity of aged tomatoes

Browning reactions occur with food processing and the thermal

Table 2
Volatile compound lists of aged tomatoes by moisture-assisted aging technology.

ID	Classification	Compound name	Formula	RT	RI	FFNSC	NIST	Odor
V1	Alcohols	2,3-Butanediol	$C_4H_{10}O_2$	5.485	825	–	803	creamy
V2		Linalool oxide II	$C_{10}H_{18}O_2$	13.719	1071	1069	1070	floral
V3		Linalool tetrahydride	$C_{10}H_{22}O$	16.014	1134	1102	–	floral
V4	Aldehydes	β-Sinensal	$C_{15}H_{22}O$	33.877	1692	1701	1694	citrus
V5		Benzaldehyde	C_7H_6O	9.711	960	960	964	almond
V6		Phenylacetaldehyde	C_8H_8O	12.617	1041	1045	1046	honey-like
V7		n-Nonaldehyde	$C_9H_{18}O$	14.913	1104	1107	1104	waxy, citrus, floral, green
V8		n-Decanal	$C_{10}H_{20}O$	18.576	1205	1208	1206	floral
V9		*trans*, *trans*-2,4-Nonadienal	$C_9H_{10}O$	18.841	1213	1218	1218	citrus
V10		β-Cyclocitral	$C_{10}H_{16}O$	18.933	1215	1201	1217	fruity, green, minty
V11		Neral	$C_{10}H_{16}O$	19.685	1237	1238	1238	lemon-like
V12	Aromatics	m-Cymene	$C_{10}H_{14}$	14.357	1089	1080	–	citrus
V13	Acids	3,5,5-Trimethylhexanoic acid	$C_9H_{18}O_2$	16.301	1142	–	1139	rancid
V14	Esters	1-Methoxy-2-propyl acetate	$C_6H_{12}O_3$	9.191	945	–	914	sweet ether-like
V15		2,3-Butanediyl diacetate	$C_8H_{14}O_4$	13.099	1055	–	1065	unnknown
V16		Linalyl anthranilate	$C_{17}H_{23}NO_2$	14.745	1099	1104	–	floral
V17		Benzyl acetate	$C_9H_{10}O_2$	16.968	1161	1167	1165	floral, fruity
V18		β-Phenethyl acetate	$C_{10}H_{12}O_2$	20.224	1253	1257	1260	floral, sweet
V19		Neryl acetate	$C_{12}H_{20}O_2$	23.789	1358	1361	1358	citrus, floral
V20		Methylbutylphenyl acetate	$C_{13}H_{18}O_2$	28.476	1505	1502	–	dairy
V21		2,2,4-Trimethyl-1,3-pentanediol diisobutyrate	$C_{11}H_{22}O$	30.885	1586	–	1587	fruity
V22		Dihydroactinidiolide	$C_9H_{12}O_2$	29.038	1524	–	1519	fruity
V23	Ketones	6-methyl-hept-5-en-2-one	$C_8H_{14}O$	10.556	984	986	–	citrus
V24		Acetoin acetate	$C_6H_{10}O_3$	13.568	1067	–	1065	fruity
V25		*trans*-Geranylacetone	$C_{13}H_{22}O$	26.643	1446	1450	1453	floral, fruit
V26		*trans*-β-Ionone	$C_{13}H_{20}O$	27.615	1477	1490	1476	floral, woody
V27		β-Ionone epoxide	$C_{13}H_{20}O_2$	27.698	1480	1489	1487	sweet, fruity, woody
V28	Phenols	Methyl salicylate	$C_8H_8O_3$	18.036	1190	1192	1191	minty
V29		m-Eugenol	$C_{10}H_{12}O_2$	23.548	1350	–	1362	spicy, pungent, clove
V30	Terpenes	Limonene	$C_{10}H_{16}$	12.156	1029	1030	1030	lemon-like
V31		Fenchyl alcohol	$C_{10}H_{18}O$	15.423	1118	1123	1121	lime-like
V32		β-*cis*-Terpineol	$C_{10}H_{18}O$	16.524	1148	1149	–	woody
V33		Bornyl alcohol	$C_{10}H_{18}O$	17.347	1171	1171	1173	camphor
V34		4-Terpinenol	$C_{10}H_{18}O$	17.653	1180	1184	1184	woody
V35		α-Terpinenol	$C_{10}H_{18}O$	18.181	1194	1195	1190	lilac
V36		Florosa	$C_{10}H_{20}O_2$	18.353	1199	1200	–	floral, sweet
V37		β-Citronellol	$C_{10}H_{20}O$	19.33	1227	1232	1228	citrus, floral
V38		Geraniol	$C_{10}H_{18}O$	20.154	1250	1255	1249	floral, lemongrass
V39		γ-Terpinenol	$C_{10}H_{18}O$	13.216	1058	1058	1058	lilac
V40	Pyrazines	Ligustrazine	$C_8H_{12}N_2$	14.207	1085	1083	1095	nutty

*Abbreviation descriptions: RT, RI, FFNSC, and NIST represented the retention time, retention index, FFNSC 3 library, and NIST 2018 library, respectively. The odor type corresponded with information from The Good Scents Company Information System (www.thegoodscentscompany.com). "– "represented no related RI of similar analysis condition was found in the library.

treatment of tomatoes leads to non-enzymatic browning reactions such as the Maillard reaction, caramelization, and ascorbic acid browning. The MAAT in this study was performed below the caramelization temperature, thereby evaluating the browning reaction model consisting mainly of the Maillard reaction and ascorbic acid browning in AT. In an acidic environment, the main intermediate MRPs were 5-HMF and furfural (Carvalho et al., 2013; Liu, Lu, Li, Zheng & Qiao, 2018). Groups UW, UD, BW, and BD were aged for 0, 3, 6, 9, and 12 days and were subjected to heatmap analysis (Fig. 5A). The columns in the heatmap were divided into four sections. From left to right, the first section was the AT from higher water activity-based tomatoes and aged for 6 to 12 days (UW-6, UW-9, UW-12, BW-6, BW-9, and BW-12), which differed significantly from the other sections ($p < 0.05$). The second section was the AT from lower water activity-based tomatoes and aged for 9 to 12 days (UD-9, UD-12, BD-9, and BD-12). The third section consisted of fresh tomatoes (UW-0 and BW-0). The fourth section consisted of all remaining groups, with no significant differences in this section ($p > 0.05$).

The composition of the AT changed during MAAT (Fig. 5A). Fresh tomatoes contained higher sucrose contents, ascorbic acid contents, and browning degree. As the aging time increased, the sucrose and ascorbic acid contents decreased significantly, while increasing contents of 5-HMF and furfural (Figs. 5B–C) (Hurtta, Pitkänen & Knuutinen, 2004). During thermal treatment with water as the reaction substrate, not only were the glycosidic bonds of sucrose hydrolyzed to glucose and fructose, but glucose was simultaneously isomerized to fructose. The non-enzymatic browning reaction accelerated when the aging parameter was set at 75% RH (Tudino, Nunes, Mandelli & Carvalho, 2020). At the same time, the water was removed by evaporation during MAAT. The HPLC-DAD analysis results showed the 5-HMF content of groups UW and BW after MAAT increased from none detected to 0.078 ± 0.016 and 0.101 ± 0.008 mg/g DW, respectively, while groups UD and BD were 0.017 ± 0.001 and 0.015 ± 0.002 mg/g DW, respectively. The ascorbic acid reduction was related to the increased furfural content due to dehydration during MAAT, with the loss of one carbon dioxide molecule and two water molecules (Wallington et al., 2013). Furthermore, the furfural content of groups UD and BD after MAAT increased from 0.009 ± 0.002 to 0.210 ± 0.001 and 0.288 ± 0.004 mg/g DW, respectively, while groups UW and BW were 0.017 ± 0.000 and 0.011 ± 0.000 mg/g DW, respectively.

When MAAT was used to develop AT, the contents of furfural, sucrose, ascorbic acid, and browning degree were all closely correlated. Meanwhile, similar correlation of fructose, glucose, and 5-HMF contents (Fig. 5A). The formation of these two MRPs (5-HMF and furfural) depended on the different water activity substrates. The first section (left of the heatmap) shows greatly reduced disaccharide (sucrose), decomposition into monosaccharides (fructose and glucose), and conversion to 5-HMF. The AT from higher water activity tomatoes (0.967–0.996) increased the deconstruction of sugars and subsequent polymerization. In addition, the rate of reducing sugar consumption was lower than its

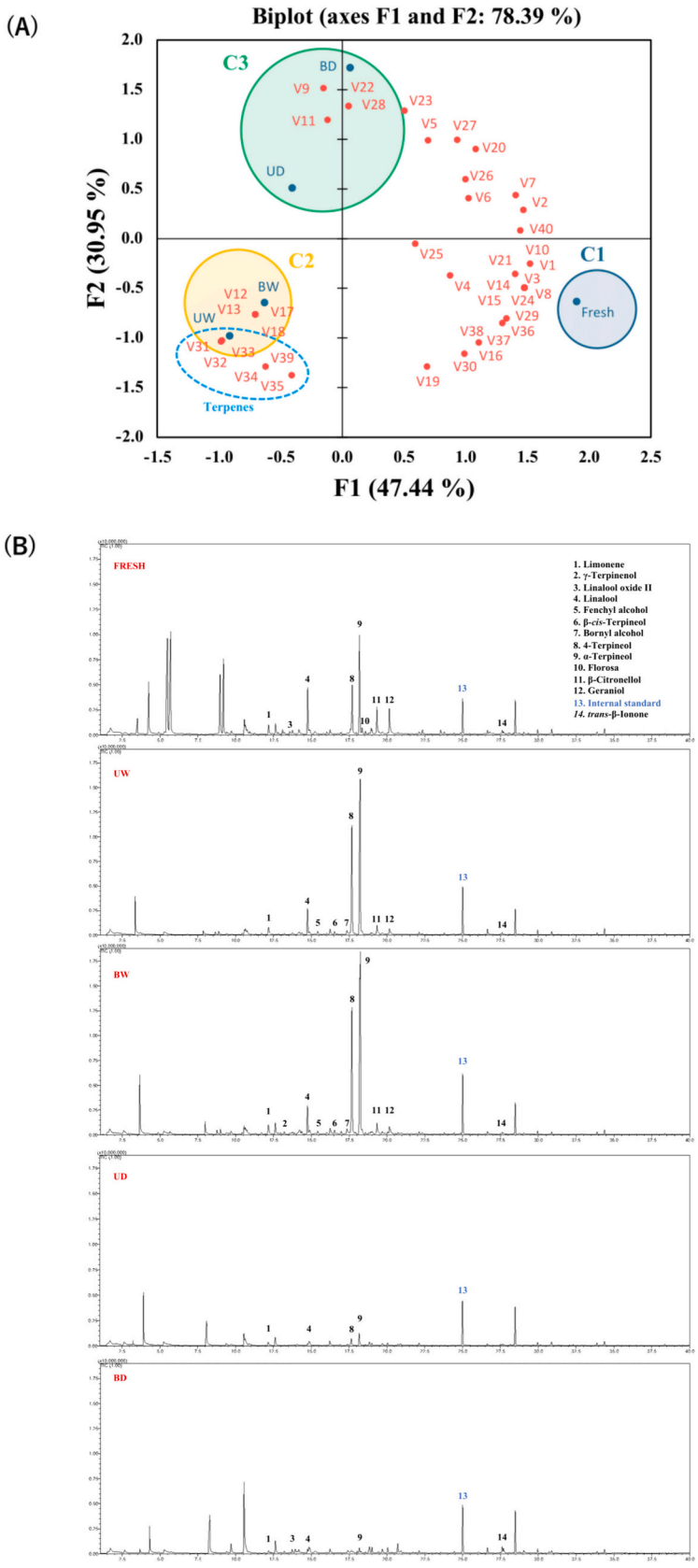

Fig. 6. Effects of volatile profiles on tomatoes during moisture-assisted aging technology. (A) Principal component analysis blots (B) Total ion chromatogram of headspace solid-phase microextraction gas chromatography–mass spectrometry analysis.
*Abbreviation description: U and B mean unblanched and blanched, respectively. W and D mean the samples used fresh or pre-dried tomatoes, respectively.

generation, resulting in a continuous increase in reducing sugar content. These results were responded to those from black garlic in previous studies, which showed that a higher relative humidity environment would significantly increase the 5-HMF content (Sun & Wang, 2018; Hsu et al., 2024). In contrast, ascorbic acid reduction and furfural formation dominated the second section. AT with less water activity (0.607–0.719) increased the oxidation of ascorbic acid and caused a level of browning that was accompanied by furfural after MAAT (Wallington et al., 2013).

3.6. Volatile profile change affected by water activity of aged tomatoes

The total volatile composition listed in Table 2 included 3 alcohols, 8 aldehydes, 1 aromatic, 1 acid, 10 esters, 5 ketones, 2 phenols, 10 terpenes, and 1 pyrazine (Table 2). In Fig. 6, PCA was used to investigate the complex metabolism of terpene and aroma production in aged tomatoes (Lin et al., 2024). Different Aw levels affected terpene formation by consuming the carotenoids (lutein, lycopene, and β-carotene) as precursors. Primary oxidation products were identified at lower Aw AT (0.607–0.719) conditions, including linalool, α-ionone, β-ionone, and β-damascenone, which contributed fruity, sweet, and woody odors. In contrast, secondary oxidation products such as limonene, fenchyl alcohol, β-cis-terpineol, bornyl alcohol, 4-terpineol, α-terpineol, and γ-terpineol were detected at higher Aw AT (0.967–0.996) and contributed lemon, woody, camphor, herbal, spicy, and clove odors (Ho, Zheng, & Li, 2015). AT is similar to tangerine peel and has a unique herbal and woody aroma (Ho et al., 2015; Zhang, Guo, et al., 2023; Zhang, Tong, et al., 2023). Briefly, terpene metabolism in AT followed different carotenoid oxidation pathways under different Aw conditions. Modulating Aw levels during processing can optimize terpene synthesis to achieve desired sensory attributes, thereby enhancing the overall consumer experience.

4. Conclusions

MAAT is a green processing technology with the advantages of no additives, low pollution, and low cost. In this study, high water activity-based tomatoes (0.967–0.996) and low water activity-based tomatoes (0.607–0.719) were aged at 65 °C and 75% relative humidity for 12 days. Through FTIR and HS-SPME GC–MS analysis, we determined the biotransformation of carotenoids, converting from esterified form to the free form and producing primary and secondary oxidation products. The generation of terpenes in aged tomatoes contributed unique aromas with a woody odor. Besides, this study discovered that the water activity of the substrate can regulate the synthesis pathway of 5-HMF or furfural, which can be used as a quality control factor for MAAT-related product development. During the browning process of aged tomatoes, as the color deepens, the total flavonoids and inhibitory α-glucosidase activity were also significantly enhanced, which has the potential to resist postprandial blood sugar. These results provide insights into the browning mechanism and functional potential of higher water activity-based aged tomatoes by MAAT, such as free from carotenoids, terpenes, and resistance to postprandial blood sugar, and can provide valuable reference for MAAT-related health and nutrition product development into the future.

CRediT authorship contribution statement

Yi-Chan Chiang: Writing – review & editing, Writing – original draft, Visualization, Validation, Methodology, Formal analysis, Data curation, Conceptualization. **Po-Yuan Chiang:** Investigation.

Declaration of competing interest

The authors declare that they have no known competing financial interests or personal relationships that could have influenced the work reported in this study.

Data availability

Data will be made available on request.

Acknowledgements

This study was supported by the National Science and Technology Council (NSTC) under Project 112-2221-E-005-014-MY2. The support of the HS-SPME GC–MS analysis from Dr. Chih-Yu Lo of National Chiayi University and FTIR measurements from the Instrument Center of National Chung Hsing University is gratefully acknowledged.

References

Ahmad, F. T., Asenstorfer, R. E., Soriano, I. R., & Mares, D. J. (2013). Effect of temperature on lutein esterification and lutein stability in wheat grain. *Journal of Cereal Science, 58*(3), 408–413. https://doi.org/10.1016/j.jcs.2013.08.004

Carvalho, A. F. A., de Oliva Neto, P., Da Silva, D. F., & Pastore, G. M. (2013). Xylo-oligosaccharides from lignocellulosic materials: Chemical structure, health benefits and production by chemical and enzymatic hydrolysis. *Food Research International, 51*(1), 75–85. https://doi.org/10.1016/j.foodres.2012.11.021

Ciou, J. Y., Chen, H. C., Chen, C. W., & Yang, K. M. (2021). Relationship between antioxidant components and oxidative stability of peanut oils as affected by roasting temperatures. *Agriculture, 11*(4), 300. https://doi.org/10.3390/agriculture11040300

Dedić, A., & Alispahic, A. (2017). Extraction and chemical characterization of lycopene from fresh and processed tomato fruit. In *Conference of 23rd International Symposium on Separation Sciences* (p. 233). https://www.researchgate.net/publication/328043676.

Gahler, S., Otto, K., & Böhm, V. (2003). Alterations of vitamin C, total phenolics, and antioxidant capacity as affected by processing tomatoes to different products. *Journal of Agricultural and Food Chemistry, 51*(27), 7962–7968. https://doi.org/10.1021/jf034743q

Gan, R. Y., Lui, W. Y., Chan, C. L., & Corke, H. (2017). Hot air drying induces browning and enhances phenolic content and antioxidant capacity in mung bean (*Vigna radiata* L.) sprouts. *Journal of Food Processing and Preservation, 41*(1), Article e12846. https://doi.org/10.1111/jfpp.12846

Gupta, R., Kopec, R. E., Schwartz, S. J., & Balasubramaniam, V. M. (2011). Combined pressure–temperature effects on carotenoid retention and bioaccessibility in tomato juice. *Journal of Agricultural and Food Chemistry, 59*(14), 7808–7817. https://doi.org/10.1021/jf200575t

Ho, C. T., Zheng, X., & Li, S. (2015). Tea aroma formation. *Food Science and Human Wellness, 4*(1), 9–27. https://doi.org/10.1016/j.fshw.2015.04.001

Hsu, T. Y., Yang, K. M., Chiang, Y. C., Lin, L. Y., & Chiang, P. Y. (2024). The Browning properties, antioxidant activity, and α-glucosidase inhibitory improvement of aged oranges (*Citrus sinensis*). *Foods, 13*(7), 1093. https://doi.org/10.3390/foods13071093

Hurtta, M., Pitkänen, I., & Knuutinen, J. (2004). Melting behaviour of D-sucrose, D-glucose and D-fructose. *Carbohydrate Research, 339*(13), 2267–2273. https://doi.org/10.1016/j.carres.2004.06.022

Iqbal, N., Hazra, D. K., Purkait, A., Agrawal, A., Saini, M. K., & Kumar, J. (2023). Eco-oriented formulation and stabilization of oil–colloidal biodelivery systems based on GC-MS/MS-profiled phytochemicals from wild tomato for long-term retention and penetration on applied surfaces for effective crop protection. *Journal of Agricultural and Food Chemistry, 71*(8), 3719–3731. https://doi.org/10.1021/acs.jafc.2c08612

Jacob, K., Garcia-Alonso, F. J., Ros, G., & Periago, M. J. (2010). Stability of carotenoids, phenolic compounds, ascorbic acid and antioxidant capacity of tomatoes during thermal processing. *Archivos Latinoamericanos de Nutrición, 60*(2), 192–198 (Google Scholar).

Jomova, K., & Valko, M. (2013). Health protective effects of carotenoids and their interactions with other biological antioxidants. *European Journal of Medicinal Chemistry, 70*, 102–110. https://doi.org/10.1016/j.ejmech.2013.09.054

Juániz, I., Ludwig, I. A., Huarte, E., Pereira-Caro, G., Moreno-Rojas, J. M., Cid, C., & De Peña, M. P. (2016). Influence of heat treatment on antioxidant capacity and (poly) phenolic compounds of selected vegetables. *Food Chemistry, 197*, 466–473. https://doi.org/10.1016/j.foodchem.2015.10.139

Khachik, F., Carvalho, L., Bernstein, P. S., Muir, G. J., Zhao, D. Y., & Katz, N. B. (2002). Chemistry, distribution, and metabolism of tomato carotenoids and their impact on human health. *Experimental Biology and Medicine, 227*(10), 845–851. https://doi.org/10.1177/153537020222701002

Koh, E., Charoenprasert, S., & Mitchell, A. E. (2012). Effects of industrial tomato paste processing on ascorbic acid, flavonoids and carotenoids and their stability over one-year storage. *Journal of the Science of Food and Agriculture, 92*(1), 23–28. https://doi.org/10.1002/jsfa.4580

Li, K., Yao, F., Xue, Q., Fan, H., Yang, L., Li, X., Sun, L., & Liu, Y. (2018). Inhibitory effects against α-glucosidase and α-amylase of the flavonoids-rich extract from *Scutellaria baicalensis* shoots and interpretation of structure–activity relationship of its eight flavonoids by a refined assign-score method. *Chemistry Central Journal, 12*(1), 1–11. https://doi.org/10.1186/s13065-018-0445-y

Li, P. H., Shih, Y. J., Lu, W. C., Huang, P. H., & Wang, C. C. R. (2023). Antioxidant, antibacterial, anti-inflammatory, and anticancer properties of *Cinnamomum*

kanehirae Hayata leaves extracts. *Arabian Journal of Chemistry, 16*(7), Article 104873. https://doi.org/10.1016/j.arabjc.2023.104873

Lin, L. Y., Chen, C. W., Chen, H. C., Chen, T. L., & Yang, K. M. (2024). Developing the procedure-enhanced model of ginger-infused sesame oil based on its flavor and functional properties. *Food Chemistry: X.* , Article 101227. https://doi.org/10.1016/j.fochx.2024.101227

Liu, P., Lu, X., Li, N., Zheng, Z., & Qiao, X. (2018). Characterization, variables, and antioxidant activity of the Maillard reaction in a fructose–histidine model system. *Molecules, 24*(1), 56. https://doi.org/10.3390/molecules24010056

Liu, S., Sun, H., Ma, G., Zhang, T., Wang, L., Pei, H., Li, X., & Gao, L. (2022). Insights into flavor and key influencing factors of Maillard reaction products: A recent update. *Frontiers in Nutrition, 9*, Article 973677. https://doi.org/10.3389/fnut.2022.973677

Lu, Q., Peng, Y., Zhu, C., & Pan, S. (2018). Effect of thermal treatment on carotenoids, flavonoids and ascorbic acid in juice of orange cv. Cara Cara. *Food Chemistry, 265*, 39–48. https://doi.org/10.1016/j.foodchem.2018.05.072

Luterotti, S., Bicanic, D., Marković, K., & Franko, M. (2015). Carotenes in processed tomato after thermal treatment. *Food Control, 48*, 67–74. https://doi.org/10.1016/j.foodcont.2014.06.004

Minguez-Mosquera, M. I., & Hornero-Mendez, D. (1994). Changes in carotenoid esterification during the fruit ripening of *Capsicum annuum* cv. Bola. *Journal of Agricultural and Food Chemistry, 42*(3), 640–644 (Google Scholar).

Mirón, I. J., Linares, C., & Díaz, J. (2023). The influence of climate change on food production and food safety. *Environmental Research, 216*, Article 114674. https://doi.org/10.1016/j.envres.2022.114674

Pakakaew, P., Phimolsiripol, Y., Taesuwan, S., Kumphune, S., Klangpetch, W., & Utama-Ang, N. (2022). The shortest innovative process for enhancing the S-allylcysteine content and antioxidant activity of black and golden garlic. *Scientific Reports, 12*(1), Article 11493. https://doi.org/10.1038/s41598-022-15635-3

Ríos-Ríos, K. L., Montilla, A., Olano, A., & Villamiel, M. (2019). Physicochemical changes and sensorial properties during black garlic elaboration: A review. *Trends in Food Science & Technology, 88*, 459–467. https://doi.org/10.1016/j.tifs.2019.04.016

Sun, Y. E., & Wang, W. (2018). Changes in nutritional and bio-functional compounds and antioxidant capacity during black garlic processing. *Journal of Food Science and Technology, 55*(2), 479–488. https://doi.org/10.1007/s13197-017-2956-2

Tsai, Y. J., Lin, L. Y., Yang, K. M., Chiang, Y. C., Chen, M. H., & Chiang, P. Y. (2021). Effects of roasting sweet potato (*Ipomoea batatas* l. lam.): Quality, volatile compound composition, and sensory evaluation. *Foods, 10*(11), 2602. https://doi.org/10.3390/foods10112602

Tudino, T. C., Nunes, R. S., Mandelli, D., & Carvalho, W. A. (2020). Influence of dimethylsulfoxide and dioxygen in the fructose conversion to 5-hydroxymethylfurfural mediated by glycerol's acidic carbon. *Frontiers in Chemistry, 8*, 263. https://doi.org/10.3389/fchem.2020.00263

Van Boekel, M. A. J. S. (2001). Kinetic aspects of the Maillard reaction: A critical review. *Food/Nahrung, 45*(3), 150–159. https://doi.org/10.1002/1521-3803(20010601)45:3<150::AID-FOOD150>3.0.CO;2-9

Wallington, N., Clark, A. C., Prenzler, P. D., Barril, C., & Scollary, G. R. (2013). The decay of ascorbic acid in a model wine system at low oxygen concentration. *Food Chemistry, 141*(3), 3139–3146. https://doi.org/10.1016/j.foodchem.2013.05.024

Wu, J., Jin, Y., & Zhang, M. (2021). Evaluation on the physicochemical and digestive properties of melanoidin from black garlic and their antioxidant activities *in vitro*. *Food Chemistry, 340*, Article 127934. https://doi.org/10.1016/j.foodchem.2020.127934

Yilmaz, Y., & Toledo, R. (2005). Antioxidant activity of water-soluble Maillard reaction products. *Food Chemistry, 93*(2), 273–278. https://doi.org/10.1016/j.foodchem.2004.09.043

Yuan, K. C., Chiang, Y. C., Li, P. H., & Chiang, P. Y. (2024). Physicochemical and release properties of anthocyanin gastric floating tablets colloidized with κ-carrageenan/metal ions. *Food Hydrocolloids, 150*, Article 109674. https://doi.org/10.1016/j.foodhyd.2023.109674

Zanoni, B., Pagliarini, E., Giovanelli, G., & Lavelli, V. (2003). Modelling the effects of thermal sterilization on the quality of tomato puree. *Journal of Food Engineering, 56*(2–3), 203–206. https://doi.org/10.1016/S0260-8774(02)00251-0

Zhang, C., Guo, X., Guo, R., Zhu, L., Qiu, X., Yu, X., Chai, J., Gu, C., & Feng, Z. (2023). Insights into the effects of extractable phenolic compounds and Maillard reaction products on the antioxidant activity of roasted wheat flours with different maturities. *Food Chemistry: X, 17*, Article 100548. https://doi.org/10.1016/j.fochx.2022.100548

Zhang, Y., Tong, X., Chen, B., Wu, S., Wang, X., Zheng, Q., … Qiao, Y. (2023). Novel application of HS-GC-IMS for characteristic fingerprints and flavor compound variations in citrus reticulatae pericarpium during storage with different *Aspergillus niger* fermentation. *Food Chemistry: X, 18*, Article 100653. https://doi.org/10.1016/j.fochx.2023.100653

Zhu, Z., Zhang, Y., Wang, W., Sun, S., Wang, J., Li, X., … Jiang, Y. (2022). Changes in physicochemical properties, volatile profiles, and antioxidant activities of black apple during high-temperature fermentation processing. *Frontiers in Nutrition, 8*, Article 794231. https://doi.org/10.3389/fnut.2021.794231